Journal of Nuclear Materials 390–391 (2009) 1039–1042

Contents lists available at ScienceDirect

Journal of Nuclear Materials

journal homepage: www.elsevier.com/locate/jnucmat

Microstructural evolution in tungsten and copper probes under hydrogen irradiation at ISTTOK

D. Nunes [a], R. Mateus [a], I.D. Nogueira [b], P.A. Carvalho [a,b,*], J.B. Correia [c], N. Shohoji [c], R.B. Gomes [a], H. Fernandes [a], C. Silva [a], N. Franco [d], E. Alves [d]

[a] Euratom/IST, Instituto de Plasmas e Fusão Nuclear, Instituto Superior Técnico, Av. Rovisco Pais, 1049-001 Lisboa, Portugal
[b] Euratom/IST, Departamento de Engenharia de Materiais, Instituto Superior Técnico, Av. Rovisco Pais, 1049-001 Lisboa, Portugal
[c] INETI, Departamento de Materiais e Tecnologias de Produção, Estrada do Paço do Lumiar, 1649-038 Lisboa, Portugal
[d] ITN, Instituto Tecnológico e Nuclear, Estrada Nacional 10, 2686-953 Sacavém, Portugal

ARTICLE INFO

PACS:
62.10.–x
66.30.jp

ABSTRACT

Commercially pure tungsten and copper wires acting as Langmuir probes to estimate edge parameters of ISTTOK plasma have been investigated for long term hydrogen migration. The microstructure of both materials revealed recrystallization and strong grain growth at the most severely exposed regions. A low number of large bubbles was observed at the most severely exposed regions, whereas a high density of small intergranular bubbles was found at more moderately exposed regions. Bubble distribution, lattice parameter, grain size, Youngs modulus and microhardness were assessed across longitudinal sections of the probes. The results indicate that bubble formation in tungsten and copper first wall components can be expected to occur and strategies for minimization of this retention phenomenon need to be implemented.

1. Introduction

The high melting point, high threshold for sputtering and low tritium inventory of tungsten render this material potentially suitable for high flux components and high-power density structural applications in fusion reactors [1]. Cu alloys are considered appropriate heat-sink materials for first wall panels due to their favorable thermal conductivity, mechanical strength and radiation resistance [2].

Energetic hydrogen ions are able to penetrate the surface barrier of metals and this ion driven permeation can exceed gas driven permeation by several orders of magnitude. The solubility of hydrogen isotopes in tungsten and copper is low and hydrogen atoms are likely to come out of solution at traps such as vacancies, voids, and grain boundaries, where they achieve a lower potential energy than that attained at crystalline sites [3]. The traps eventually become saturated and, even for the low neutral gas pressure in the fusion chamber, untrapped hydrogen atoms diffuse out of the implant zone deeper into the material. At the saturated traps, molecular recombination tends to occur resulting in bubbles and blisters with increasing internal pressure. At enhanced diffusivity conditions the system can reduce the interfacial free energy by bubble and blister coarsening.

Analysis of tungsten performance as a plasma-facing material and its damage by hydrogen plasmas is currently underway [1,3]. Crucial for a deeper comprehension of these characteristics is the settling of basic hydrogen migration parameters and the establishment of a complete description of trapping/retention mechanisms. In fact, trapping mechanisms and retention have been evaluated only in tungsten foils [4–9] or thin films [10], which hinders a complete description of retention in bulk materials, where bubbles and blisters can be expected to play a crucial role. Hydrogen permeation through the plasma-facing materials is expected to condition the performance of non-plasma-facing materials at the first wall. Hence, further studies on the microstructural evolution of first wall materials seem necessary [11].

In the present work, the microstructure of tungsten and copper wires exposed to low energy proton irradiation at low pressure have been investigated for long term hydrogen migration characteristics.

2. Experimental procedure

Commercially pure W (99.95%, 0.75 mm diameter) and Cu (>99.99%, 2 mm diameter) wires have been exposed at the ISTTOK tokamak edge plasma for ~200 discharges of 30 ms with time intervals of 10 min in 10^{-4} torr H_2 atmospheres. The W wire was

* Corresponding author. Address: Departamento de Engenharia de Materiais, Instituto Superior Técnico, Av. Rovisco Pais, 1049-001 Lisboa, Portugal.
E-mail address: pac@ist.utl.pt (P.A. Carvalho).

0022-3115/$ - see front matter © 2009 Elsevier B.V. All rights reserved.
doi:10.1016/j.jnucmat.2009.01.283

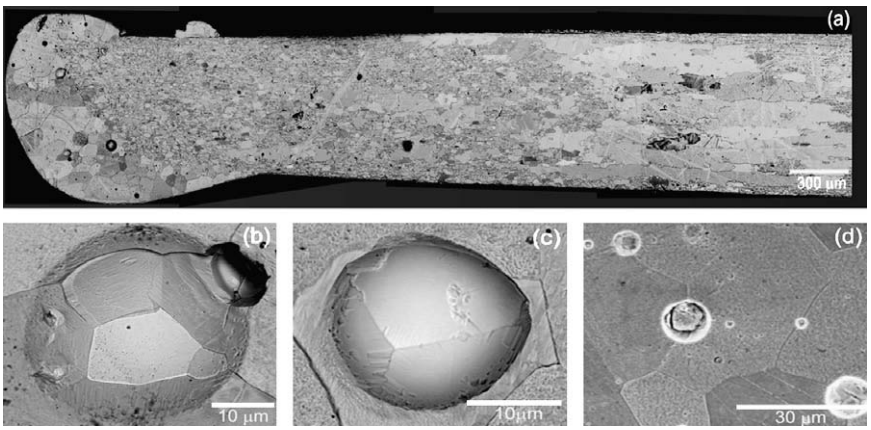

Fig. 1. (a) Microstructure of the W probe, (b and c) large bubbles and (d) intergranular bubbles.

oriented radially with an exposure length of 3 mm while the Cu wire was oriented vertically with an exposure length of 20 mm (all the Cu wire was exposed). The wires position was varied from discharge to discharge across the ISTTOK edge plasma (up to 2 cm inside the limiter position). The plasma parameters were: electron and ion temperature, $T_e \sim T_i = 15–50$ eV, density, $n = 0.5–2.10^{18}$ m^{-3}, hydrogen flux, $\Gamma^{H+} = 1–7 \times 10^{22}$ m^{-2}s^{-1}, and fluence lower than 4.10^{23} particles/m^2.

Longitudinal sections of the W and Cu wires were investigated up to, respectively, 12.5 mm and 8 mm from the probe edge. Microstructural observations were carried out by optical and scanning electron microscopy after standard metallographic preparation. The grain size ($\sqrt{A}$) was determined from the average grain area (A) using the Jeffries planimetric method. X-ray diffraction experiments were performed using a Rigaku DMAX-III C microdiffractometer under Bragg–Brentano geometry with $K_{\alpha 1}$ radiation and a 0.6 mm probe diameter. Lattice parameters were determined by the least squares method using the $\cos^2\theta/\sin\theta$ extrapolation function with the respective $(211)_W$, $(220)_W$, $(310)_W$, $(321)_W$ and $(220)_{Cu}$, $(311)_{Cu}$, $(222)_{Cu}$ reflections collected at each point. Hardness and Young's modulus variations were assessed through force–displacement plots obtained with a Shimadzu DUH-W201S ultramicrohardness tester, using a Berkovich indenter, a load of 1 N and a hold time at peak load of 20 s.

3. Results and discussion

After irradiation the probes shape exhibited changes that point to strong softening, incipient melting and/or evaporation (Figs. 1(a) and 2(a)). The microstructures of both materials evidence recrystallization and abnormal grain growth (Figs. 1(a) and 2(a)). Recrystallization was more pronounced for Cu. However W underwent a less uniform grain variation across the longitudinal section. A large number of recrystallization twins were present in the Cu grains.

In spite of the moderate H^+ fluence and irradiation energy of the ions, these have migrated inwards and severe bubble nucleation occurred at internal grain boundaries. This suggests that these defects act initially as traps and subsequently as hydrogen recombination sinks [12]. Nevertheless, the highly coherent mirror planes separating twinned regions in the Cu probe do not constitute nucleation sites for bubbles (Fig. 2(d)). A higher density of small intergranular bubbles was found at moderately exposed regions (Figs. 1(d) and 2(d)), while a lower number of large intergranular bubbles was present at the most severely exposed regions (as large

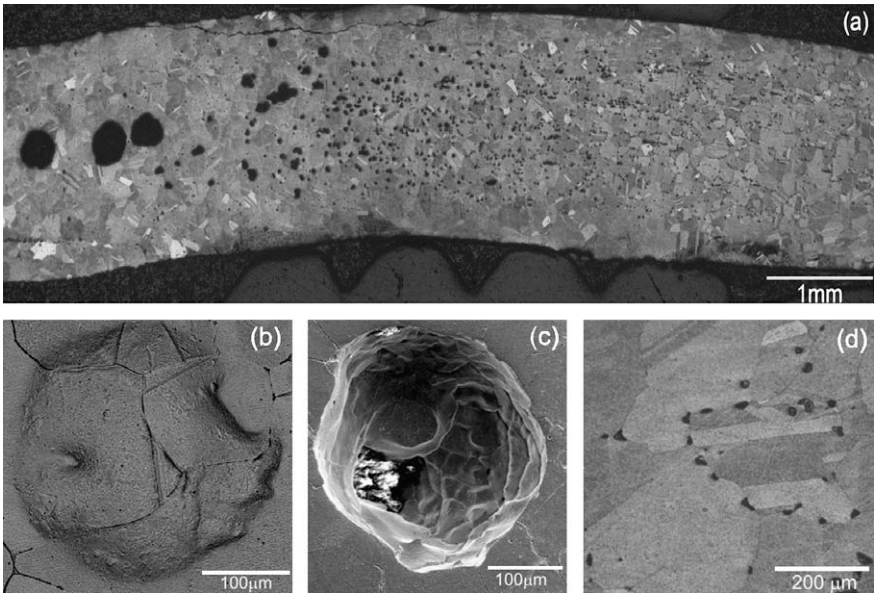

Fig. 2. (a) Microstructure of the Cu probe, (b and c) large bubbles, and (d) intergranular bubbles.

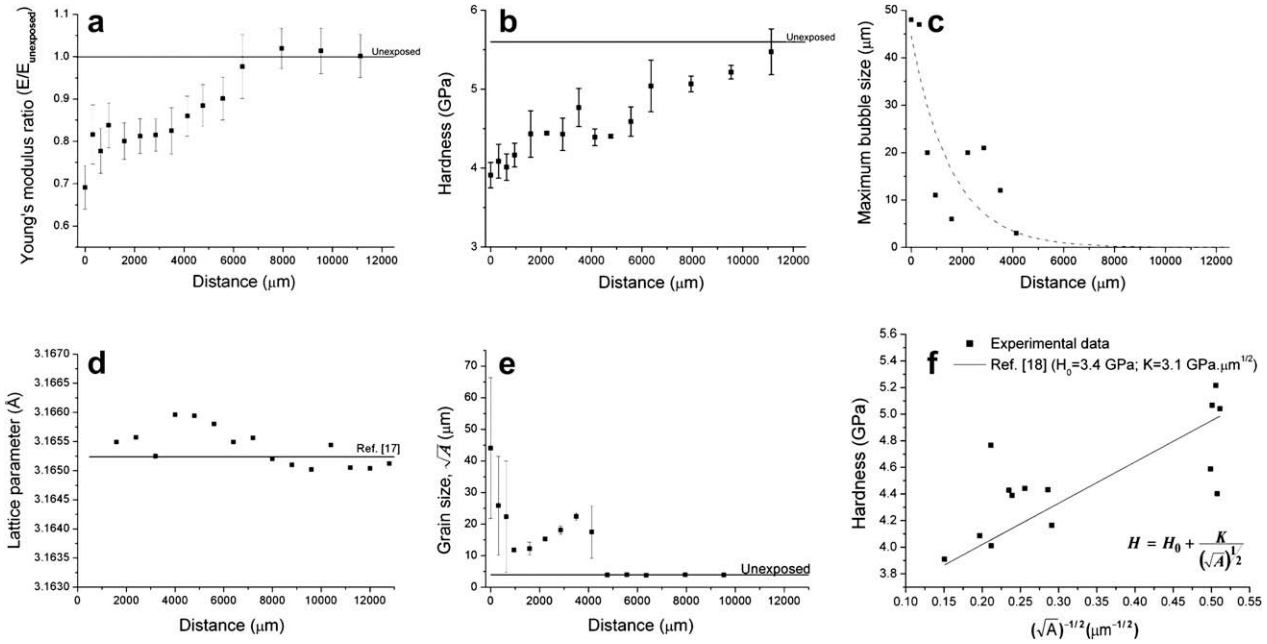

Fig. 3. (a) Young's modulus, (b) hardness, (c), maximum bubble size variation, (d) lattice parameter, (e) grain size, and (f) relation between hardness and grain size for W. (See above-mentioned references for further information).

as 50 μm in W, Fig. 1(b and c), and 300 μm in Cu, Fig. 2 (b and c)). This bubble distribution indicates that large bubbles result from a coarsening process which is particularly evident within the Cu probe: at least exposed regions small bubbles are homogeneously distributed at the grain boundaries across the probe thickness, whereas at the probe edge only large central bubbles could be found. This suggests that at initial exposure stages, smaller and scattered bubbles have been formed at the probe edge, which over time coarsened through an Ostwald ripening mechanism [13] into the large bubbles observed in the center (the apparent bubble migration span is then as high as 1 mm). Nucleation of high pressure bubbles at grain boundaries and their coalescence seem closely associated with the recrystallization process and indicate that retention studies should consider the grain size distribution and its evolution over time.

Figs. 3 and 4 present the Young's modulus (a), hardness (b), maximum bubble size variations (c), lattice parameter (d) and grain size (e) across longitudinal sections of the W and Cu probes, as well as the relation between hardness and grain size (f). The most severely exposed regions exhibit a significant decrease both in Young's modulus and hardness when compared to unexposed materials (Figs. 3(a and b) and 4(a and b)). This can be essentially justified by the higher porosity level [14] and larger grain size [15,16], respectively.

The lattice parameter variation for W points to higher hydrogen saturation at the intermediate regions and lower saturation at the

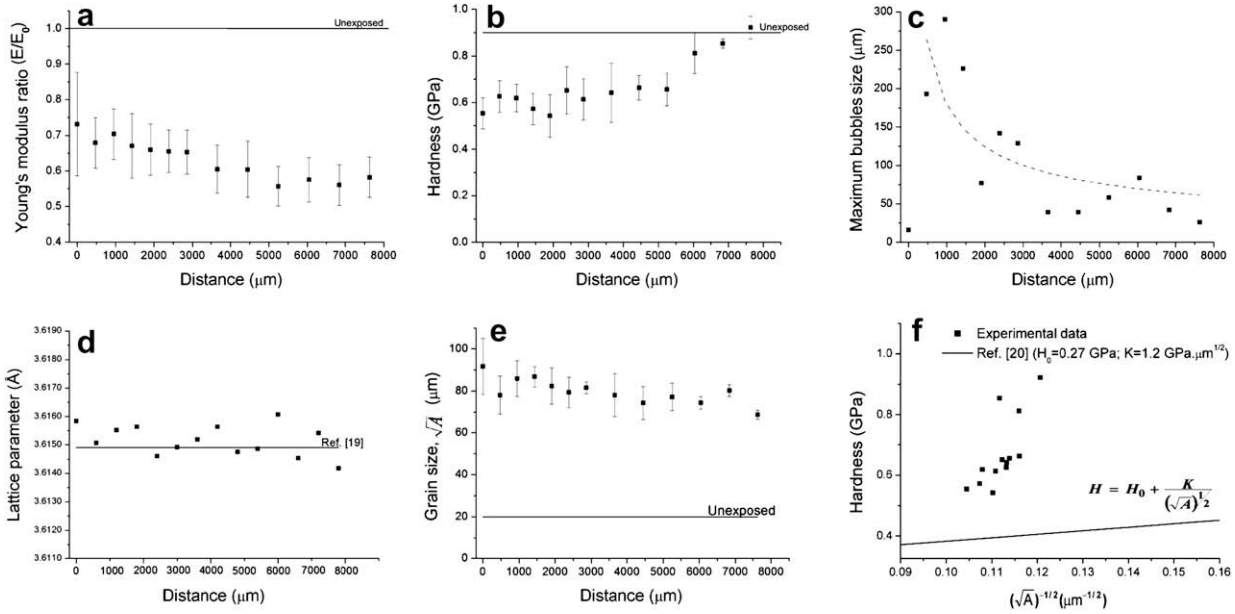

Fig. 4. (a) Young's modulus, (b) hardness, (c), maximum bubble size variation, (d) lattice parameter, (e) grain size, and (f) relation between hardness and grain size for Cu. (See above-mentioned references for further information).

probe edge. The Young's modulus variation for W shows a correlation with the lattice parameter (Fig. 3(a and d)) and is also expected to depend on the porosity level [14]. The grain size variation of this probe (Fig. 3 (e)) reflects the irregular growth behavior observed in the microstructure (Fig. 1(a)). Hardness follows a linear Hall–Petch dependence on grain size (Fig. 3(f)). This indicates that under the present irradiation conditions, hardness measurements provide a suitable diagnostic of grain growth.

The large bubble size in the Cu probe hindered adequate evaluation of the Young's modulus and hardness variations (Fig. 4(a and b)), since at the coarser regions the microindentations had to be performed on individual (or few) grains around large bubbles. No trend could be inferred from the Cu lattice parameter variation (Fig. 4(d)). However, the severe porosity is expected to have contributed for an increased error in the lattice parameter determination by inducing irregular sample height in X-ray experiments. The hardness vs. grain size relation for Cu follows a linear relation (Fig. 4(f)); the discrepancy with the reported Hall–Petch parameters [20] can be mitigated if twins are considered in the grain size definition [21].

4. Conclusions

Severe bubble formation occurred at the grain boundaries of Cu and W probes exposed to edge plasma at ISTTOK at low H^+ fluence and low irradiation energies. Bubble coarsening results in a significant (apparent) bubble migration.

Microstructural investigations involving trapping mechanisms, grain size distribution and recrystallization behavior are required for hydrogen retention studies.

Acknowledgements

This work has been carried out within the Contract of Association between EURATOM and Instituto Superior Técnico. Financial support was also received from Fundação para a Ciência e Tecnologia in the frame of the Associated Laboratory Contract.

References

[1] N. Baluc et al., Nucl. Fus. 47 (2007) S697.
[2] R. Andreani, M. Gasparotto, Fus. Eng. Des. 61/62 (2002) 27.
[3] R.A. Causey, T.J. Venhaus, Phys. Scr. T94 (2001) 9.
[4] R.A. Anderl, D.F. Holland, G.R. Longhurst, R.J. Pawelko, C.L. Trybus, C.H. Sellers, Fus. Tech. 21 (1992) 745.
[5] A.A. Haasz, M. Poon, J.W. Davis, J. Nucl. Mater. 266–269 (1999) 520.
[6] V. Alimov, K. Ertl, J. Roth, J. Nucl. Mater. 290–293 (2001) 389.
[7] D.A. Komarov, A. Markin, S. Yu, A.P. Zakharov, J. Nucl. Mater. 290 (2001) 433.
[8] F.C. Sze, R.P. Doerner, S. Luckhardt, J. Nucl. Mater. 264 (1999) 89.
[9] R. Sakamoto, T. Muroga, N. Yoshida, J. Nucl. Mater. 233–237 (1996) 776.
[10] R. Sakamoto, T. Muroga, N. Yoshida, J. Nucl. Mater. 220–222 (1995) 819.
[11] I. Mukouda, Y. Shimomura, T. Iiyama, Y. Harada, Y. Katano, T. Kakazawa, D. Yamaki, K. Noda, J. Nucl. Mater. 283–287 (2000) 302.
[12] Y. Minyou, Plasma Sci. Tech. 7 (2005) 2828.
[13] R. Delamore, E. Ntsoenzok, F. Labohm, A. Van Veen, J. Grisolia, A. Claverie, Nucl. Instrum. and Meth. B 186 (2002) 324.
[14] J.C. Wang, J. Mater. Sci. 19 (1984) 801.
[15] E.O. Hall, Proc. Phys. Soc. B64 (1951) 747.
[16] N.J. Petch, J. Iron Steel Inst. 147 (1953) 5.
[17] W. Parrish, Acta Cryst. 13 (1960) 838.
[18] Erik Lassner, Wolf-Dieter Schubert, Tungsten: Properties, Chemistry, Technology of the Element, Alloys and Chemical Compounds, Springer, 1999, p. 20, W. Parrish, Acta Cryst. 13 (1960) 838–850.
[19] M.E. Straumanis, L.S. Yu, Acta Cryst. A25 (1969) 676.
[20] V.Y. Gertsman, M. Hoffmann, H. Leiter, R. Birringer, Acta Metall. Mater. 42 (1994) 3539.
[21] J. Schiotz, Scr. Mater. 51 (2004) 837.